6.2 Study of Gasoline Pre-chamber combustion at Lean Operation

Noritaka Kimura, Hiroki Kobayashi, Naohiro Ishikawa

Abstract

Regulations and other demands to enhance automobile fuel economy are growing increasingly strict to reduce CO_2 as a measure to address the issues of global warming. The goal of this study was to enhance the fuel economy in high-load operation of a gasoline engine for hybrid vehicles, which is a useful means of addressing this issue. Technology for achieving lean combustion in high-load operation was studied to realize higher brake thermal efficiency by increasing the ratio of specific heat compared to theoretical air-fuel ratio (stoichiometric) EGR combustion. Issues for applying lean combustion to high-load operation include 1) the increased oxygen molarity results in increased knocking tendency compared to stoichiometric EGR combustion, and 2) increased leanness results in greater combustion variation due to the ignition delay period and the delayed second half of the combustion period. In order to solve these issues at lean operation, several combustion methods are examined on test bench. In this test study, Pre-chamber stratified combustion has an advantage of lean operation performance. Ignitability and high-speed combustion period of pre-chamber combustion was secured by setting the ignition areas inside the pre-chamber to the rich side relative to the total air-fuel ratio (A/F). NOx emissions are an issue for stratified combustion, but NOx emissions can be reduced by setting the pre-chamber A/F to approximately 23 and by making the pre-chamber volume sufficiently small compared to the main combustion chamber volume. Tests were performed using a single-cylinder engine to determine the pre-chamber volume and the diameter and number of jet nozzles. The pre-chamber volume and the diameter and number of jet nozzles were set under the restriction of dP/dθ, which is the index of combustion noise, as the target value or less. This specification realized minimum advance for the best torque (MBT) operation with an A/F of 35 at 2000 rpm, IMEP 810 kPa. The heat release characteristics of pre-chamber combustion shows that unlike the typical combustion pattern using strong flow, the heat release characteristics have two peaks. The first peak is the flame state wherein the jet flame has spread throughout the entire combustion chamber. This shows that the amount of heat released inside the pre-chamber enabled the flame jets from the jet nozzles to spread within the main combustion chamber. The second peak is the state wherein the unburned gas around the spread jet flames is all burning instantaneously. This combustion state results in rapid and stable combustion during the second half of combustion. This combustion characteristic realized MBT lean combustion in high-load operation. The balance between the compression ratio and the surface volume ratio (S/V) was reviewed to counter the drop in efficiency due to the increased S/V as a result of adding a pre-chamber, and this enabled MBT operation at 2000 rpm, IMEP 870 kPa, A/F 35 with an IMEP variation rate of 1.2 %, a main combustion period of 18 deg, and NOx of 30 ppm. Together with the effects of heat insulation coating inside the pre-chamber, this enhanced the brake thermal efficiency by +2 point compared to stoichiometric EGR combustion.

1   Introduction

Action to reduce emissions of CO_2, thought to be a cause of climate change, has been advancing in recent years. While the electrification of vehicles is advancing, hybrid vehicles, using a combination of internal combustion engine and electric motors, are expected to be the mainstream for the time being. For the internal combustion engine of a hybrid vehicle to make the most of an operating condition of good thermal efficiency, ongoing effort is necessary to broaden that range and further raise thermal efficiency within it.

2   Target of This Research

In raising efficiency at the most efficient point for a hybrid vehicle engine, Tagishi et al. [1] have raised brake thermal efficiency to the equivalent of 45% in a Miller Cycle gasoline engine using cooled EGR combustion at the theoretical air-fuel ratio (stoichiometric) and stroke/bore ratio (S/B) of 1.5, with late inlet valve close timing (IVC). The specifications of this engine are shown in Table 1 as ENG_A. Working towards 50% brake thermal efficiency as the next step, the targets are set to raise thermal efficiency three points, through waste heat recovery and heat loss reduction technology, and achieving the remaining two points by increasing the ratio of specific heat. This research studied the lean combustion as a means of raising theoretical thermal efficiency compared to stoichiometric EGR, through improved ratio of specific heat. For target air-fuel ratio (A/F), Fig. 1 shows the resulting change in brake thermal efficiency calculated for EGR combustion and lean operating conditions, using a 1D simulation of a case with minimum advance for best torque (MBT) and main combustion period (MFB 10-90%) fixed at 25 deg. It was stipulated that at least A/F 28 was necessary to attain the 2 points of thermal efficiency.
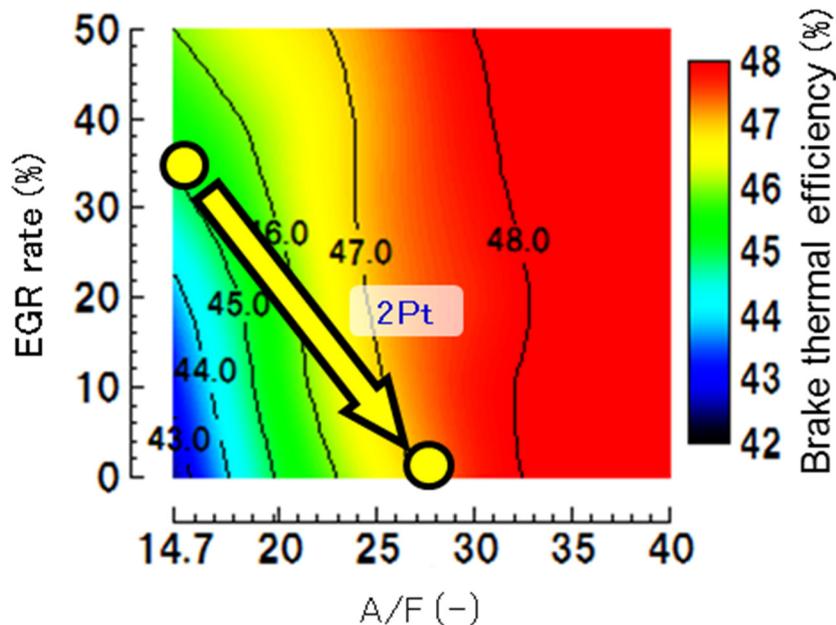

Figure 1: Brake thermal efficiency on EGR combustion and lean combustion using 1-D simulation

The test engine under assessment was the ENG_B single cylinder engine shown in Table 1. This engine was intended to replace future hybrid engines, and had S/B of 1.5, based on the research results from Tagishi et al.

Table 1: Test engine specifications of pre-chamber combustion

	ENG_A	ENG_B
Bore (mm)	81	73
Stroke (mm)	121.6	109.5
Stroke Bore ratio	1.5	
Displacement (cm^3)	627	458
Compression ratio	17	
Effective compression ratio	12.5	
Intake port	Tumble port	Filling port
Tumble ratio	1.8	0.4
Main fuel supply	DI	PI / DI
Ignition energy (mJ)	450	60
Air supply	Super charged	

3   Issue of Lean Combustion under High Load

3.1   Knocking Performance

The ignition timing at knocking event was retarded at the same dilution rate by changing the dilution gas from EGR to air. Figure 2 shows the MFB 50% crank angle against dilution rate by EGR and air at 2,000 rpm and IMEP of 810 kPa. With dilution with air at the same 35% as EGR dilution, the knocking ignition timing was retarded by at least 12 deg from MBT. Therefore, the thermal efficiency declined, despite of the increased ratio of specific heat due to air dilution. That appears to be due to promotion of the oxidation reaction due to elevation of the oxygen mole fraction, caused by replacement of EGR by air as the dilution gas [2]. To raise thermal efficiency in lean combustion under high load, it is necessary to achieve reduction of knocking tendency on a par with EGR combustion.
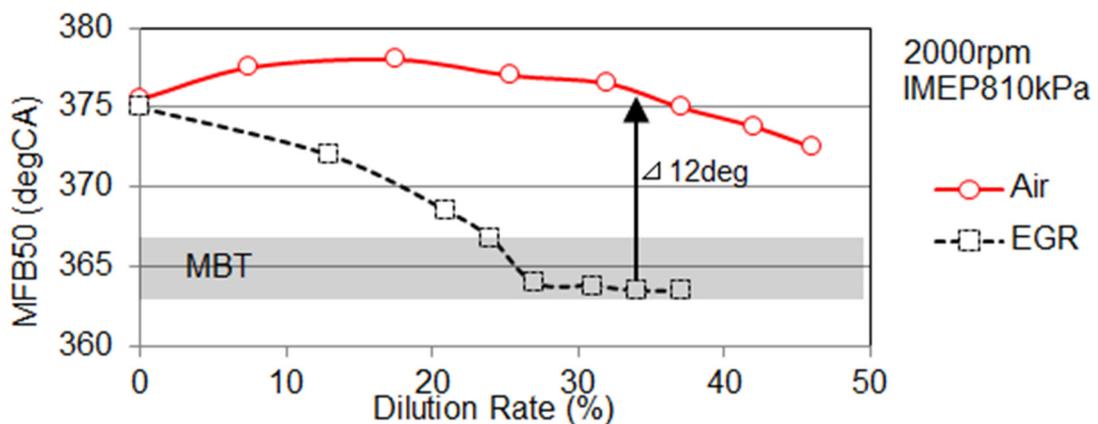

Figure 2: Effect of dilution rate to MFB 50% characteristics

3.2   Lean Limit Performance

Figure 3 shows the lean limit characteristics and combustion period at IMEP 600 kPa, which allows MBT operation. Operation at above A/F 30 is not possible under the combination of in-cylinder flow and high energy ignition that attained EGR 35%. That appears to be the case because of greater combustion variation due to the ignition delay period (IG-MFB2%), and the delayed second half of the combustion period (MFB50-90%). Ignition delay and second half combustion period should be shortened in order to extend the lean limit A/F.
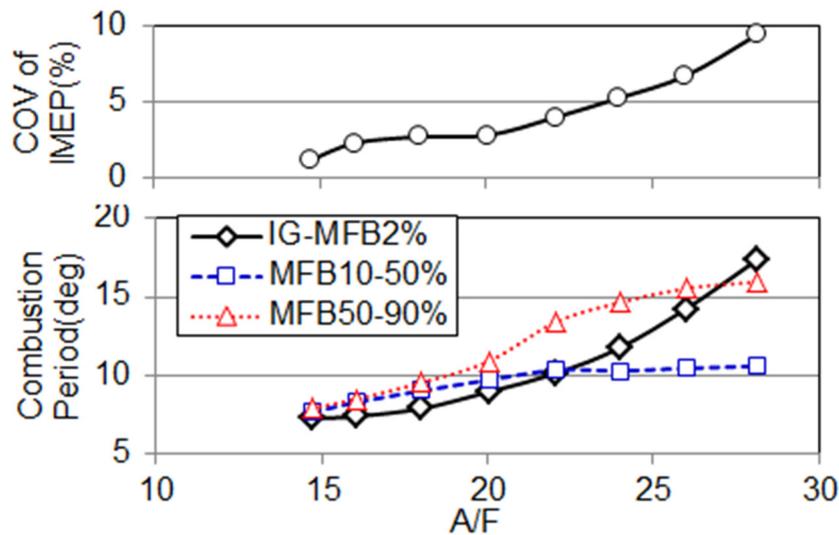
Figure 3: Combustion characteristics

4   Combustion Concept

4.1   Pre-Chamber Combustion Concept

Pre-chamber combustion, which is one of the stratified charge combustion, was researched as a solution for the above issue. Figure 4 shows the engine configuration for pre-chamber combustion. A pre-chamber is provided in the center of the combustion chamber and equipped with a spark plug, and with dedicated direct injection (DI), in order to set A/F in the pre-chamber richer than main combustion chamber A/F. Furthermore, a port injector (PI) supplies a lean fuel-air mixture. In the second half of the compression stroke, part of the lean fuel-air mixture in the main combustion chamber side flows into the pre-chamber, so that the A/F at ignition is determined by the mixture of that flow with the fuel-air mixture generated in the pre-chamber by injection within it. Figure 5 shows the combustion mode, as calculated by CFD. Ignition causes combustion inside the pre-chamber, and pressure inside the pre-chamber rises (Fig. 5①). The pressure differential between the pre-chamber and the main combustion chamber causes jet flame to spread into the main combustion chamber (Fig. 5②) and burn the lean fuel-air mixture in the main combustion chamber (Fig. 5③).
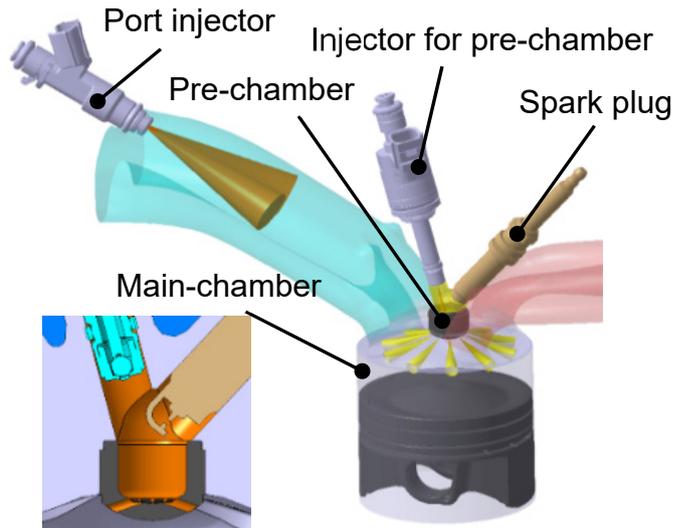
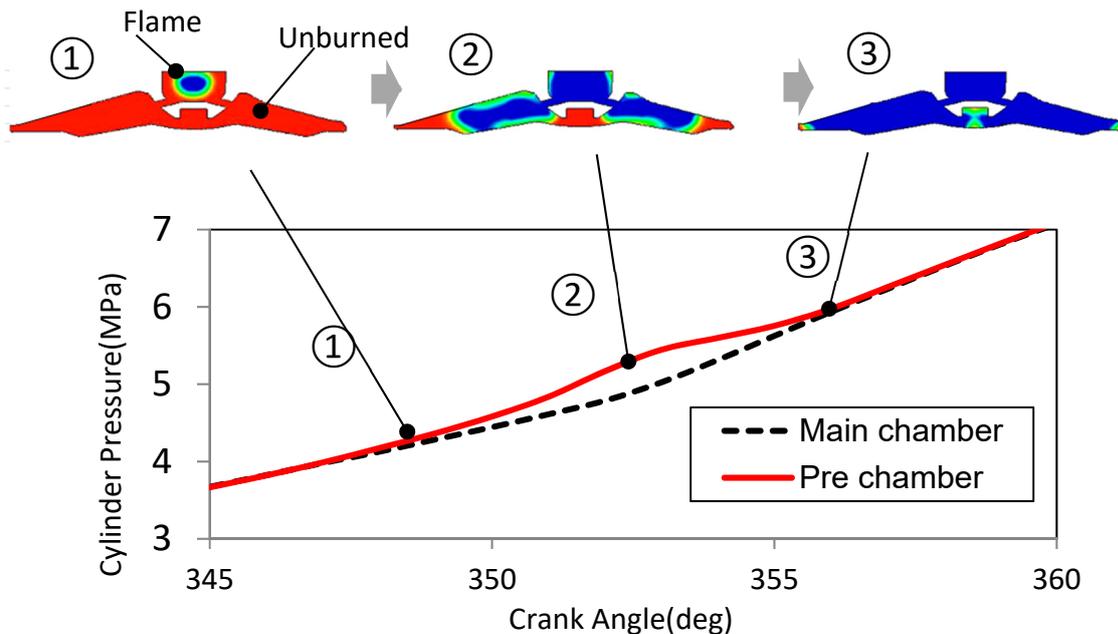*Figure 4: Engine configuration of pre-chamber combustion*

Figure 5: Pre-chamber combustion process at 2000rpm IMEP810kPa

4.2   Stratified Combustion Issues and Responses

NOx emission, an issue of stratified combustion, was approached as described below. Figure 6 shows the trend of NOx emission against A/F. This indicates that the highest value of NOx occurs close to A/F 17, and that almost no emission generate at A/F 27 or above. In stratified combustion using DI in a conventional SI engine, the setting is close to the stoichiometric level [3], out of consideration of factors such as cycle variation of A/F around the spark plug, so highly localized NOx emission from that area has been an issue. For pre-chamber combustion, the NOx target is set at 50 ppm or less

on the assumption of the use of an after treatment system for lean combustion [4] under efficiency point load. The A/F target is set in the pre-chamber close to 23, and set in the main combustion chamber at 36 or more. The reduction in NOx emission achieved was examined by keeping the pre-chamber volume 5-10% relative to the main combustion chamber. Figure 7 shows the calculated values of NOx emission for each pre-chamber volume against pre-chamber internal A/F. It was considered possible to reduce NOx emission to 50 ppm or less by using an appropriate pre-chamber volume and setting 23 as the pre-chamber internal A/F.
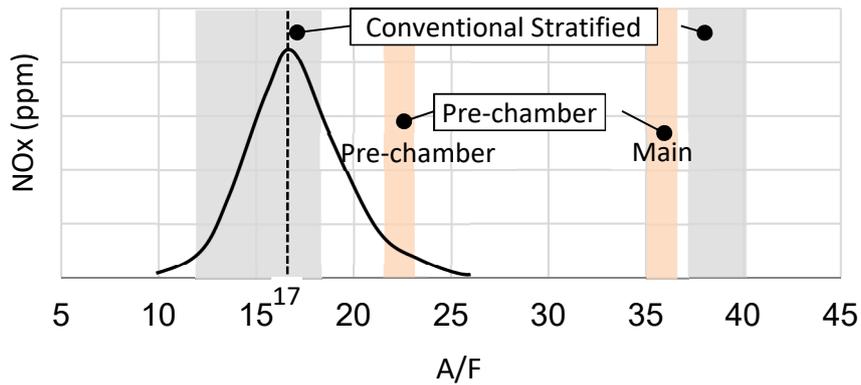

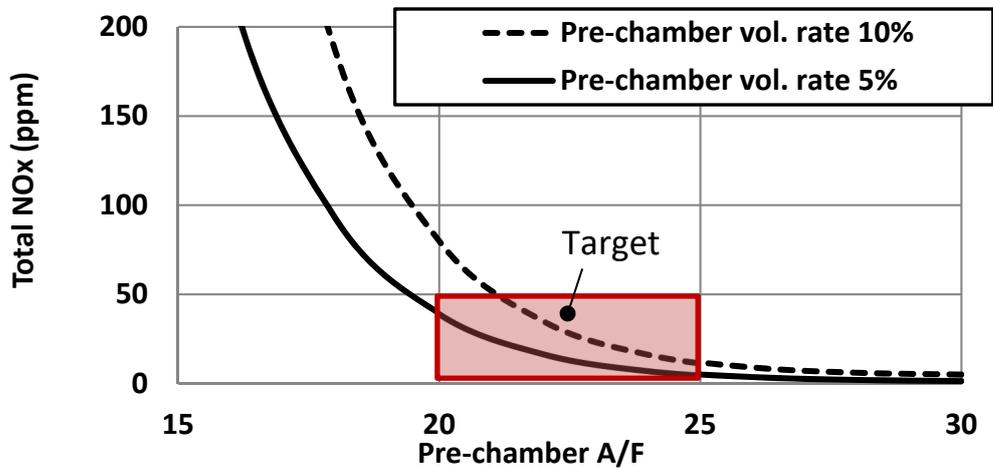Figure 6: Stratified concept of Pre-chamber combustion

Figure 7: Relation of pre-chamber A/F, Vol and NOx

4.3   Setting Pre-chamber Specifications

The pre-chamber specifications have a major impact on main-chamber combustion. Figure 8 shows the main design parameters for the pre-chamber. The sensitivity of pre-chamber volume, number of pre-chamber nozzles, nozzle diameter, and nozzle cross-sectional area calculated from nozzle diameter and number of nozzles were confirmed. The direction of the jet was set to a direction that avoids heat losses to the combustion chamber wall and piston surface.
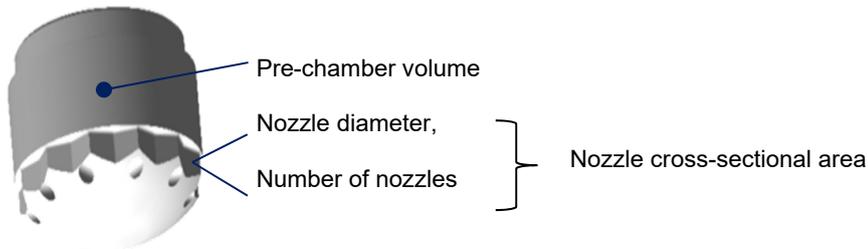
Figure 8: Design parameters of pre-chamber

Figure 9 shows NOx emission against pre-chamber volume, dP/dθ, which is an index of combustion noise, and the characteristics of main combustion period and thermal efficiency, under operating conditions of 2,000 rpm engine speed and IMEP 810 kPa, and A/F 35. A maximum was set for dP/dθ, which is an indicator of combustion noise, from the characteristic of shorter combustion period in the pre-chamber. The smaller the pre-chamber volume, the more the NOx emission and dP/dθ can be reduced, but there is a tendency for the combustion period of MFB 10-90% to increase. Results found no loss of thermal efficiency with pre-chamber volume up to 2.0 cm^3, but reduced thermal efficiency with further volume reduction. That appears to be the case because as pre-chamber volume is reduced, the proportion of rich fuel-air mixture is also reduced, which reduces NOx. At the same time, the amount of thermal energy provided from the pre-chamber to the main chamber is reduced because there is less mixture in the pre-chamber, which appears to reduce dP/dθ and increase combustion period. The change in thermal efficiency appears to be a reduction because, under A/F 35 operating conditions, the thermal energy supplied from the pre-chamber to the main chamber cannot maintain combustion stability. From the above performance results, the pre-chamber volume was set at 2.0 cm^3, which minimizes NOx emission and dP/dθ without reducing thermal efficiency.
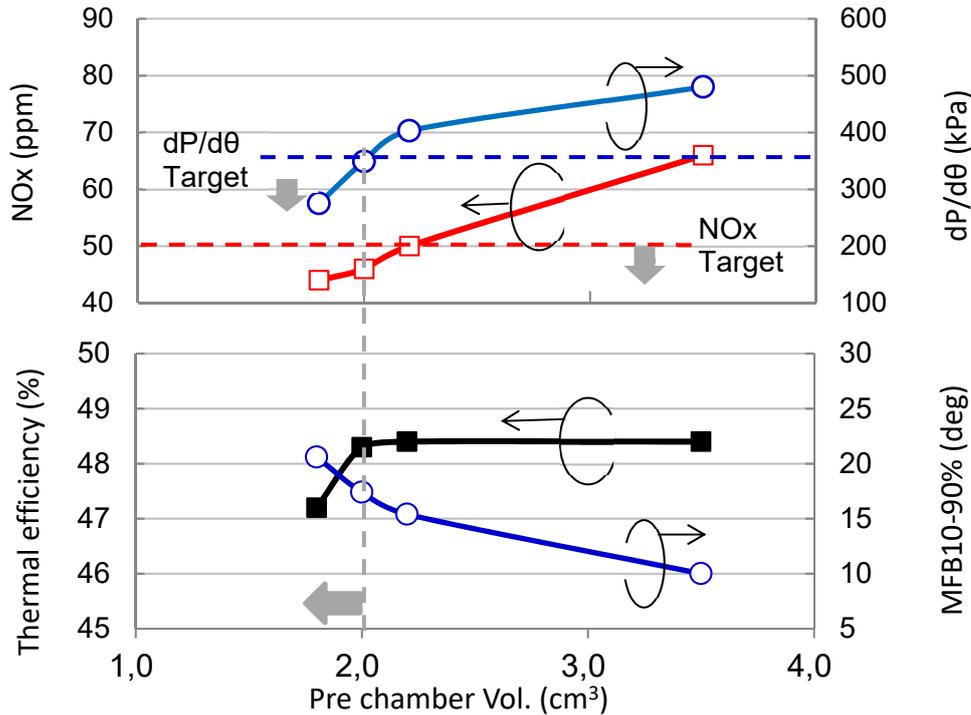
Figure 9: Comparison of pre-chamber volume on NOx and thermal efficiency

Figure 10 shows performance characteristics with variation of total cross-sectional area of pre-chamber nozzles with pre-chamber volume of 2.0 cm^3 and under operating conditions of 2,000 rpm engine speed, IMEP 810 kPa, and A/F 35. The smaller the total cross-sectional area of pre-chamber nozzles, the more NOx emission can be reduced, but dP/dθ rises. The combustion period of MFB 10-90% reduces as total cross-sectional area of pre-chamber nozzles is reduced, but thermal efficiency peaks when total cross-sectional area of pre-chamber nozzles is 20 mm^2, declining when the area is smaller or larger. That means that the smaller the total cross-sectional area of pre-chamber nozzles, the higher the pressure increase in the pre-chamber, and the higher the thermal energy supplied to the main chamber, so that combustion stability can be obtained. Therefore, it becomes possible to retard the MBT ignition timing while obtaining equal combustion stability, so that peak in-cylinder temperature is lower and NOx emission can be reduced. It appears that the change in thermal efficiency is a reduction because when total cross-sectional area of pre-chamber nozzles is above 20 mm^2, the rise in pre-chamber pressure is lower, so less thermal energy is supplied from the pre-chamber to the main chamber. Therefore, it becomes impossible to maintain combustion stability under A/F 35 operating conditions, and thermal efficiency declines. If the total cross-sectional area of pre-chamber nozzles is reduced, on the other hand, pressure in the pre-chamber rises, and thermal energy supplied to the main chamber is increased, but there is increased heat loss in the pre-chamber itself, and thermal efficiency declines. Here, we set optimal total cross section area was set as 20 mm^2, at which dP/dθ is at or below the target value and thermal efficiency is maximized. The specific design values were set at 10 pre-chamber nozzles and Φ1.6 mm as the pre-chamber nozzle diameter.
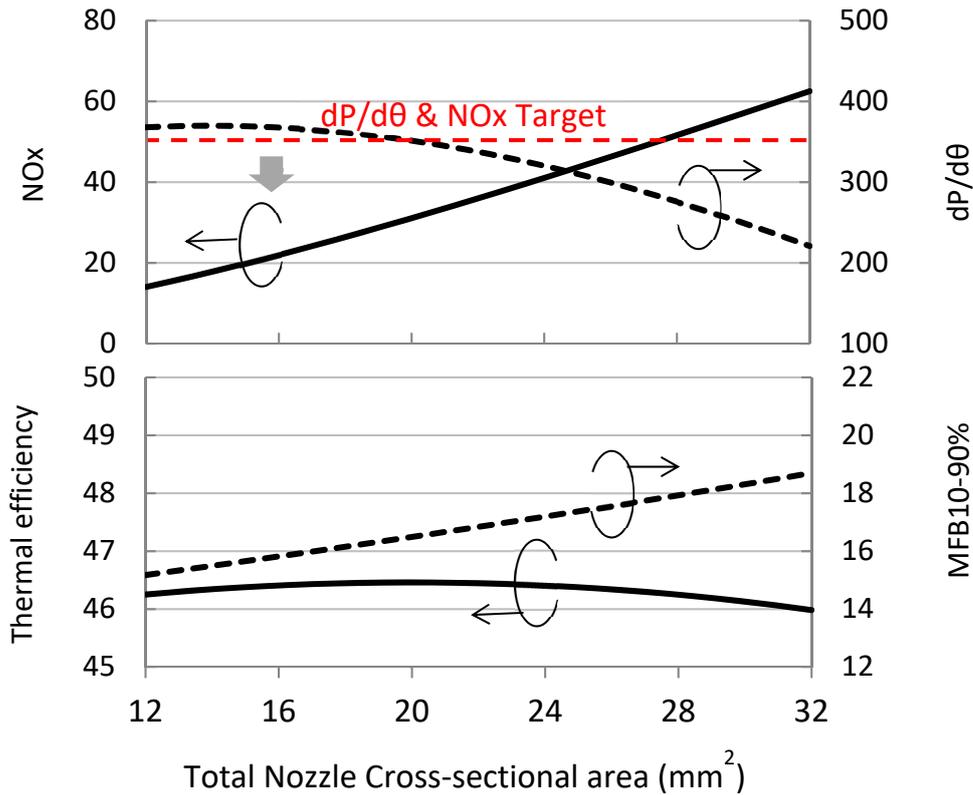
Figure 10: Comparison of total nozzle cross-sectional area on NOx and thermal efficiency

Figure 11 shows performance after optimized setting of the pre-chamber. It presents various performance results against A/F under high load operating conditions of 2,000 rpm engine speed and IMEP 810 kPa. Combustion stability was attained at COV of IMEPi 3% or less up to A/F 38. It was also confirmed that under conditions of A/F 30 or higher, the MFB 50% crank angle, which indicates knocking level, achieved MBT operation, producing a major reduction in knocking compared to homogeneous lean operation.
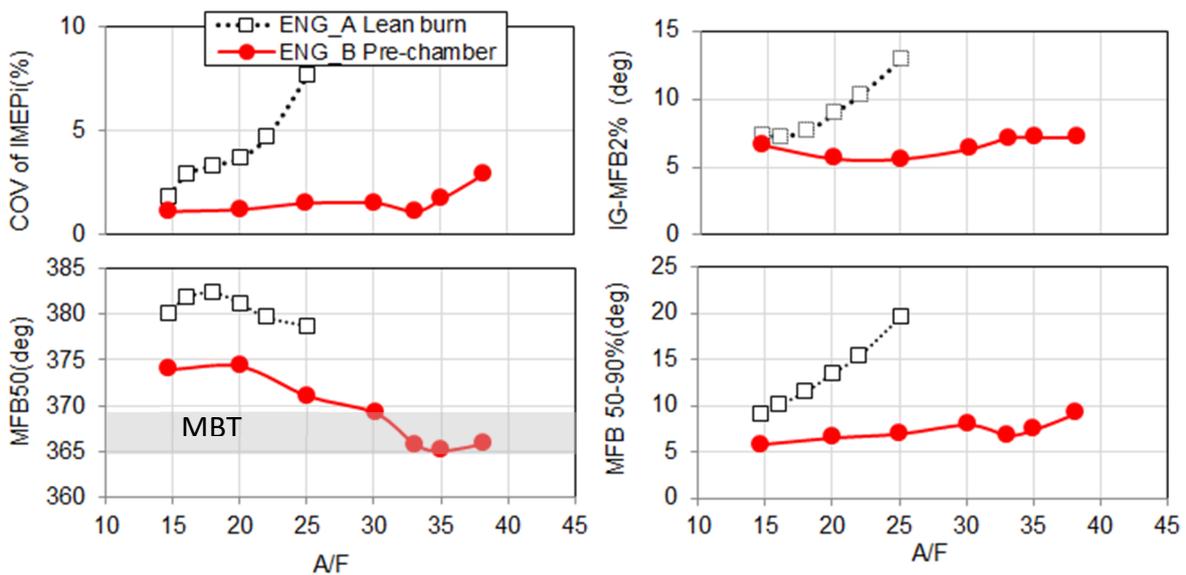

Figure 11: Lean characteristics of pre-chamber combustion

Figure 12 shows the mass fraction of burned fuel (MFB) at EGR35% for ENG_A with A/F 35 combustion by pre-chamber combustion at ENG_B, and the non-dimensional value ndQ/dθ of dQ/dθ at the gross calorific value. Pre-chamber combustions, and particularly second-half combustion after MFB 50, are rapid, and reference to ndQ/dθ shows a combustion mode with two peaks. Combustion visualization was used in order to directly observe this phenomenon. Figure 12 also shows a bottom-view flame visualization image. The state of combustion at the first peak in Fig. 12① is the time at which the jet flame from the nozzle has just spread into the combustion chamber. It can be seen that the jet flame decelerates at that time, and then volumetric ignition in the surrounding area causes the heat release in Fig. 12②. The characteristics of each combustion phase are as follows:

① The heat generation of the gas in the pre-chamber is thought to cause the jet flame to propagate into the main chamber, and flame is able to spread throughout the combustion chamber, even if the fuel-air mixture in the main combustion chamber is lean. This accelerates the initial combustion.

② The quantities of heat held by each of the multiple propagated jet flames causes instantaneous combustion of unburned areas around each jet flame, accelerating second-half combustion and reducing combustion variation.

To summarize, setting the pre-chamber A/F to around 23 shortens the ignition delay in lean pre-chamber combustion, and heat release inside the pre-chamber causes the jet flames from the nozzles to propagate into the main combustion chamber. After that, the lean fuel-air mixture around each jet flame burns instantaneously, making second-half combustion faster. This produces a stable combustion.
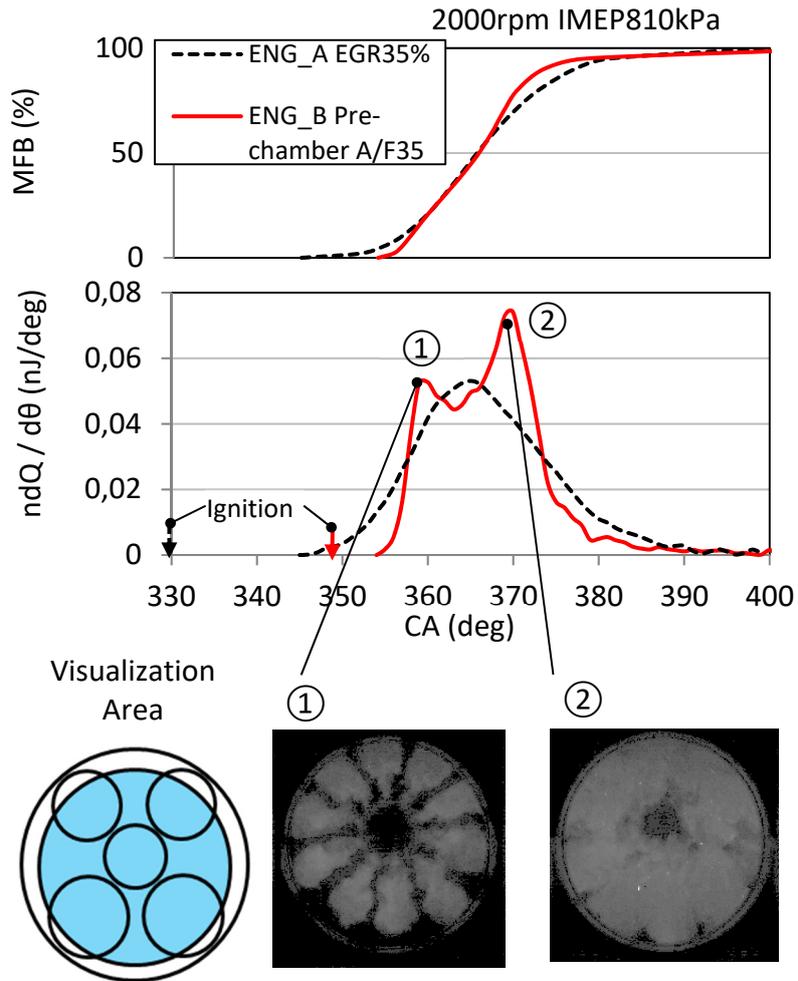
Figure 12: Combustion characteristics and flame visualization of Pre-chamber combustion

4.4   Technologies to Reduce Heat Losses in the Pre-chamber

The surface area to volume ratio (S/V) has a major influence on combustion within the pre-chamber, and the pre-chamber is thought to increase heat losses to the walls, so the reduction of heat losses within the pre-chamber was addressed. In order to reduce heat losses, a coating of insulative material was applied on the inner walls of the pre-chamber, covering the area indicated in red in Figure 13. The proportion of surface area covered was 37%. An insulative material with thermal conductivity of less than 1 W/mK was applied with a thickness of 500um. Thermal conductivity of base pre-chamber material is less 26 W/mK. Figure 14 shows performance results under operating conditions of 2,000 rpm engine speed, IMEP 810 kPa, and A/F 35. The results indicated a reduction of 0.8 points in heat loss, and an improvement of 0.5 points in thermal efficiency.

Coating area
Thermal Conductivity < 1 W/mK
Thickness 500um
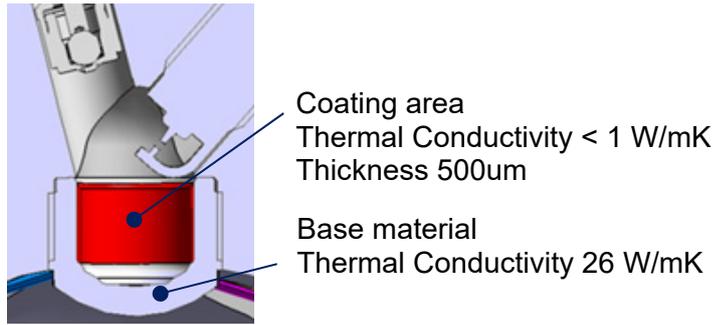
Base material
Thermal Conductivity 26 W/mK

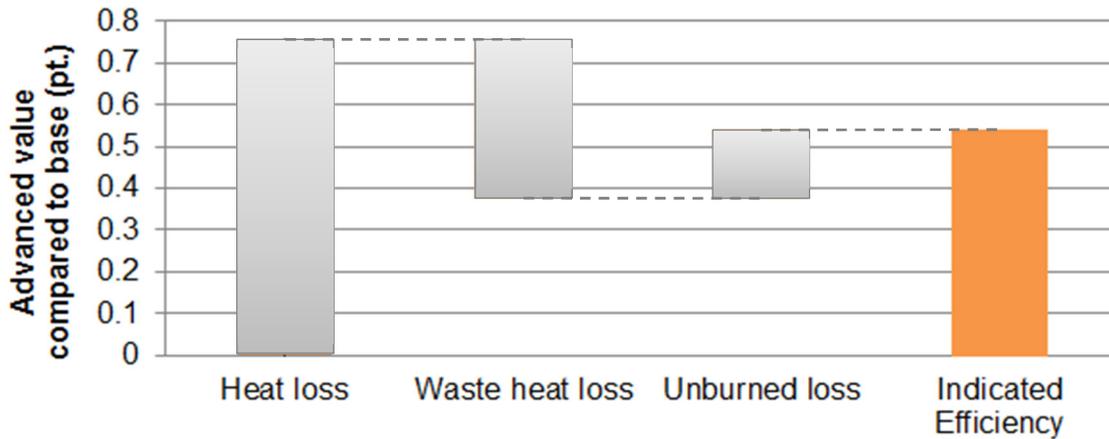*Figure 13: Thermal insulation coating area of pre-chamber*

Figure 14: Effects of insulation coating on pre-chamber

4.5   Combustion Chamber S/V Setting

In a pre-chamber combustion engine, the combustion chamber S/V is much higher than in a regular gasoline engine. For a given pre-chamber volume, this impact increases with compression ratio. Therefore, the relationship between compression ratio and combustion chamber S/V was studied. Figure 15 shows the thermal efficiency sensitivity map obtained from comparative tests of compression ratio and S/V. As Step 1 in the diagram, it was confirmed the performance of reducing combustion chamber S/V by lowering the compression ratio, in order to check the influence of combustion chamber S/V. Results obtained indicated that, while lowering compression ratio reduced theoretical thermal efficiency, thermal efficiency was actually improved because of large effects in reducing heat losses and unburned fuel losses. As Step 2 in the diagram, it was shown that thermal efficiency improving by optimizing the shape of the combustion chamber and further reducing combustion chamber S/V. Based on the above results, the compression ratio setting for the pre-chamber combustion engine was reviewed, including the shape of the combustion chamber, and set 16 as the compression ratio.
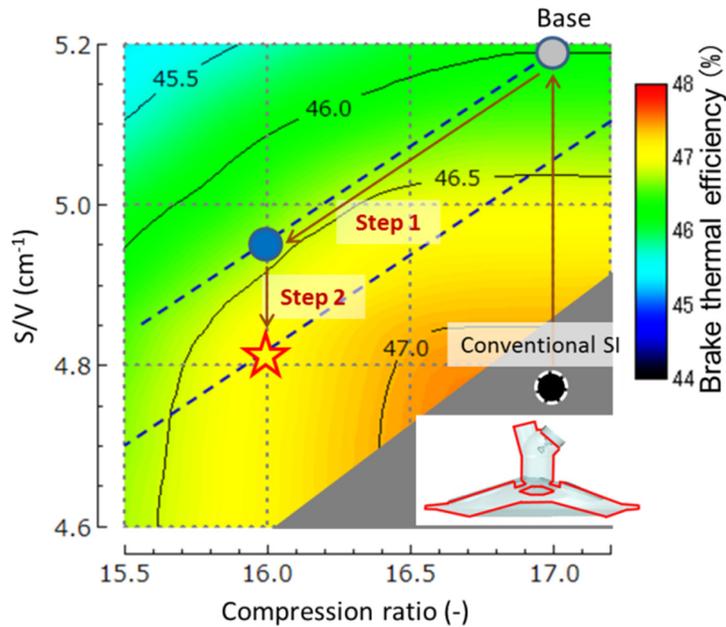
Figure 15: Effects of S/V and compression ratio on brake thermal efficiency of pre-chamber combustion engine

4.6   In-cylinder Flow Setting

The in-cylinder flow setting for the ENG_A which achieved 45% brake thermal efficiency was a high tumble port setting, intended to raise the flame propagation speed. However, in pre-chamber combustion, the combustion mode changes, so it appeared that the required in-cylinder flow setting would also change. Figure 16 shows the results of a comparison of performance between two port specifications with different tumble ratios. The tumble ratio of port A is 0.4, and that of port B is 1.8, and the results are for operating conditions of 2,000 rpm engine speed and IMEP 510 kPa. Results of the performance comparison indicate that the difference in tumble ratio causes no change in combustion period, and that combustion stability was reduced with the port B specification, which has a higher tumble ratio. The reason why there was no change in combustion period appeared to be that, in pre-chamber combustion, the presence of the spark plug in the pre-chamber means that enhanced flow does not promote initial flame kernel growth as it normally does in an spark-ignition engine. Figure 17 shows the results of subsequent analysis of in-cylinder flow by CFD, to analyze the loss of combustion stability. It shows the in-cylinder flow speed distribution at a crank angle of 80 deg before top dead center (BTDC) in the compression stroke, after fuel injection in the pre-chamber and velocity of the gas flow through the nozzle of pre-chamber. It can be seen that there is almost no gas exchange between the main chamber and the pre-chamber at port A, but there is remaining tumble flow at port B, causing gas exchange between the main chamber and the pre-chamber. Fuel which was injected in the compression stroke through a dedicated DI injector within the pre-chamber, in order to retain it within the pre-chamber, flows into the main chamber due to this residual tumble flow, so that the amount of fuel in the pre-chamber at the start of combustion changes for each cycle. As a result, it appears that the thermal energy supplied from the pre-chamber to the main chamber also varies for each cycle, as does combustion in the main chamber, reducing combustion stability. From the above, Port A with the

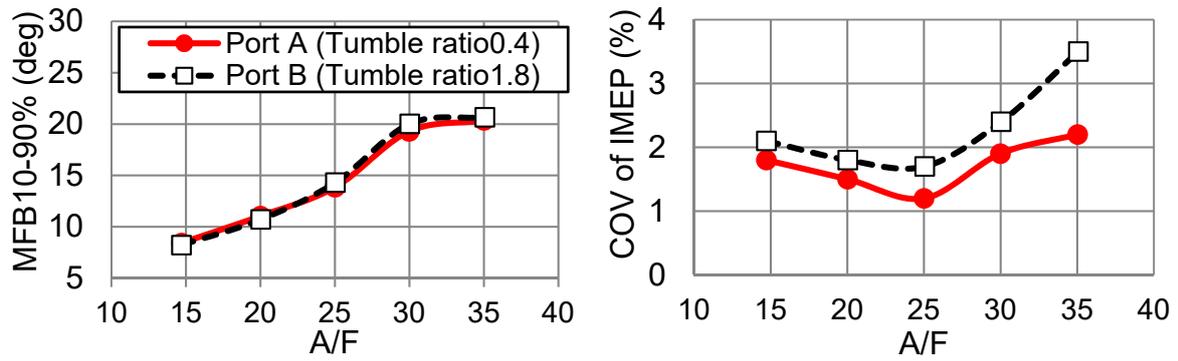lower tumble ratio was selected for the Pre-chamber combustion in-cylinder flow specifications.

Figure 16: Performance result of Intake ports with different tumble ratios
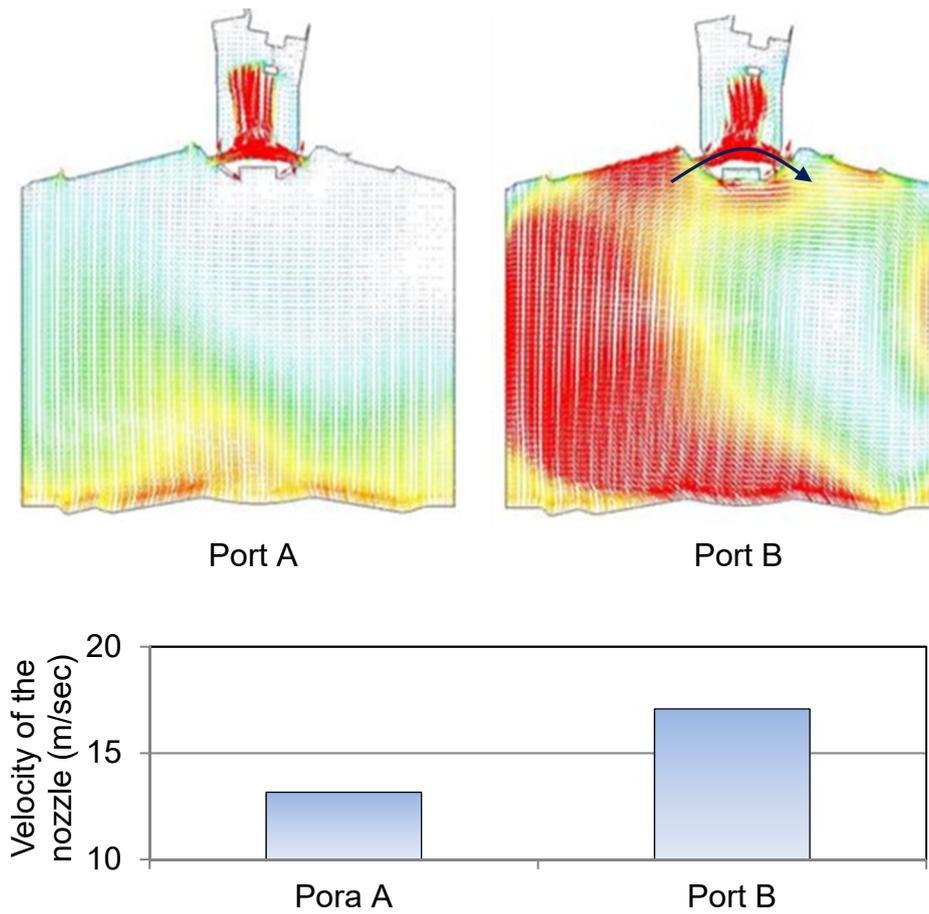

Port A   Port B

Figure 17: In-cylinder flow by CFD at crank angle 80 degBTDC

5   Results

Confirmation of the final value was attained in a single-cylinder engine which applies to all the pre-chamber combustion engine technologies described above. Table 2 shows the final engine specifications. The calculation of brake thermal efficiency used mechanical friction equivalent to an in-line four-cylinder engine the same as that used in the research which attained 45% brake thermal efficiency, and supercharger losses estimated by 1D simulation.

Table 2: Final test engine specifications

Number of cylinders	1
Displacement volume (cm^3)	458
Bore (mm)	73
Stroke (mm)	109.5
Stroke Bore ratio	1.5
Compression ratio	16
Effective compression ratio	12.5
Pre-chamber volume (cm3)	2
Nozzle diameter (mm)	1.6
Number of nozzles	10
Pre-chamber specification	Thermal insulation coating
Intake port	Filling port
Tumble ratio	0.8
Air supply	Super charged
Fuel supply (main / pre)	PI / DI
Ignition energy (mJ)	60

Figure 18 shows performance results against A/F under high load operating conditions of 2,000 rpm engine speed and IMEP of 870 kPa. Figure 19 shows a breakdown of the brake thermal efficiency improvement compared to ENG_A at EGR35%. Combustion stability attained COV of IMEP3% or less up to A/F 40, and MBT operation was achieved at A/F 35, attaining a 2-point improvement compared to 45% brake thermal efficiency. At the same time, NOx emission of 30 ppm was attained under the A/F 35 conditions at which the brake thermal efficiency improvement was attained.
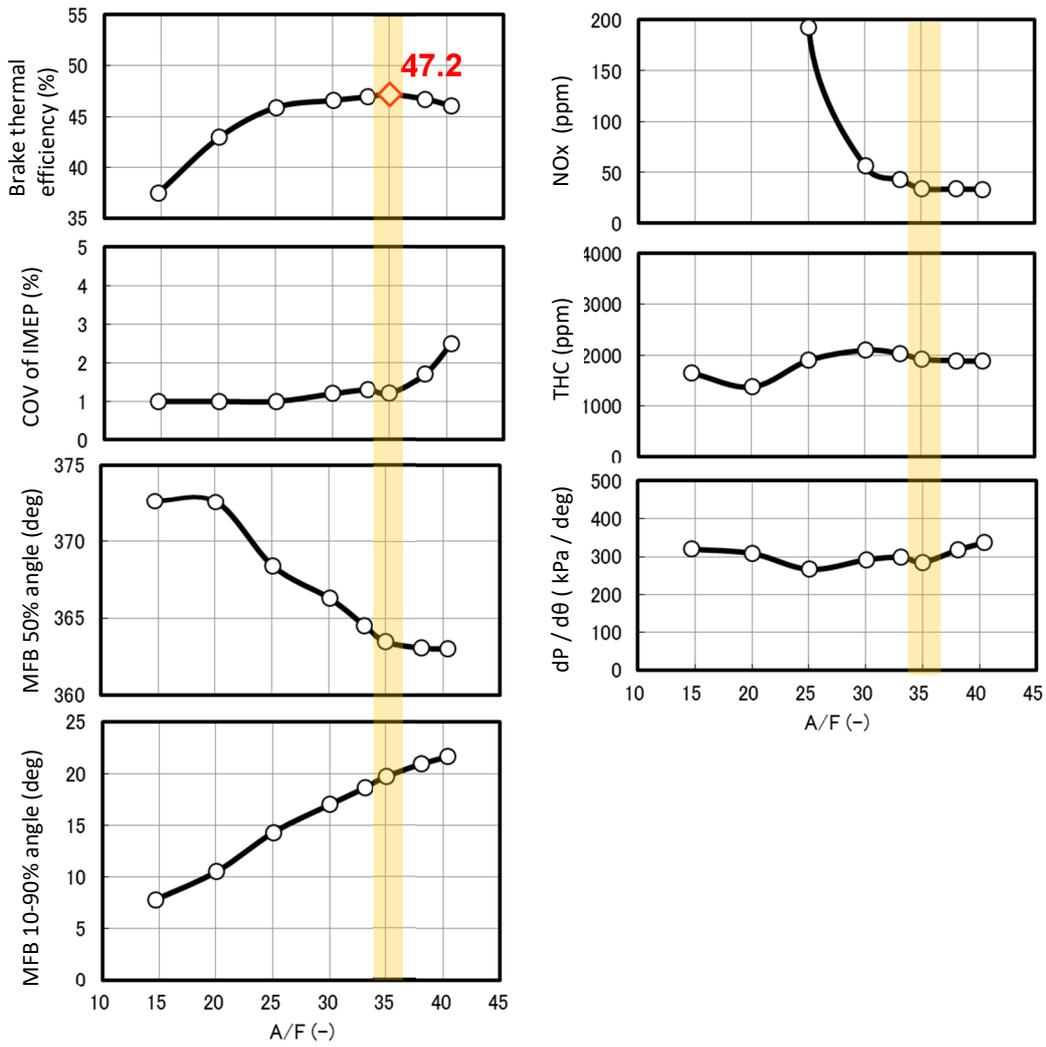
Figure 18: Lean characteristics of high load by test engine specifications
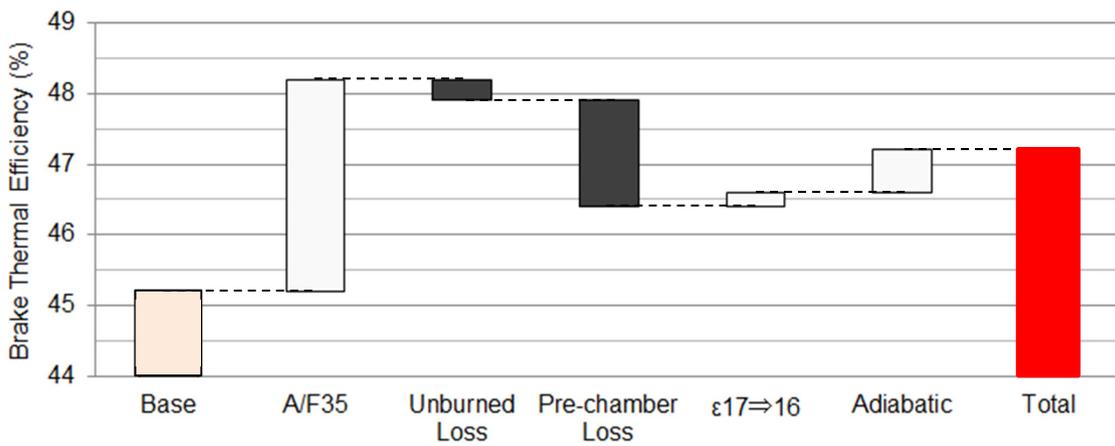

Figure 19: The influence of pre-chamber combustion at engine speed 2,000 rpm IMEP 870 kPa

6   Summary

The research of lean combustion using pre-chamber combustion obtained the following results:

(1) Brake thermal efficiency attained +2 points in comparison to ENG_A, which attained 45% brake thermal efficiency under stoichiometric EGR conditions. NOx under these conditions was below the target value.

(2) In a single-cylinder engine with a mechanical compression ratio of 16, optimization of pre-chamber design and reduction of various losses associated with the addition of a pre-chamber enable stable MBT operation at A/F 35, with 2,000 rpm engine speed and IMEP 870 kPa.

This research was validated on a single-cylinder engine. Hereafter, toward practical applications in a multi-cylinder engine for automobiles applying these achievements, two outstanding topics for future study are development of a supercharger system able to combine partial load with power point operation, and development of catalyst adapted to lean burn combustion.

Literature

[1]   Tagishi, R., Ikeya, K., Takazawa, M., Yamada, K.: In Pursuit of Thermal Efficiency in Gasoline Engines, Proceedings of the Society Of Automotive Engineers Of Japan, No.121-14, (2014)

[2]   Nakata, K., Nogawa, S., Takahashi, D., Yoshihara, Y., Kumagai, A., Suzuki, T.: Engine Technologies for Achieving 45% Thermal Efficiency of S.I. Engine, SAE Technical Paper 2015-01-1896, doi:10. 4271/2015-01-1896, (201)

[3]   Abe, S., Ishikawa, N., Tekeda, N., Akimoto, S., Matsuura, H.: Optimization of Combustion Chamber for Direct Injection Gasoline Engine Employing Center Injection System, Society of Automotive Engineers of Japan, No. 2004-08-0448

[4]   Takeori, H., Wada, K., Matsuo, Y., Morita, T., Konomoto, T., Murata, Y., Kimura, M., Miyauchi, A.: Study of an Aftertreatment System for HLSI Lean-burn Engine, SAE Technical Paper 2018-01-0945, doi:10.4271/2018-01-0945, (2018)